Two optical emission components with different variability in V404 Cygni

Y. Tachibana[1], T. Yoshii[1], H. Hanayama[2], and N. Kawai[1]

[1] Department of Physics, Tokyo Institute of Technology, 2-12-1, Ookayama, Tokyo, Japan
[2] Ishigakijima Astronomical Observatory, National Astronomical Observatory of Japan, Ishigaki, Okinawa, Japan
E-mail(YT): tachibana@hp.phys.titech.ac.jp

Abstract

In this paper, we report the multi-color optical observation of V404 Cygni at the beginning of its 2015 outburst performed by the MITSuME and MURIKABUSHI telescopes. With time domain analysis of the multi-color light curves, we successfully decomposed optical variations into two components: a highly-variable, and a less-variable component. The loci of the less-variable component in the color-color diagram are consistent with that of multi-color blackbody radiation, while those of the highly-variable component trace out those of power-law spectra with spectral indices $\alpha \sim 0.6$–1.0. For the less-variable component, we argue that an irradiated disk with the innermost temperature higher than $\sim 2.0 \times 10^4$ K and the outermost temperature lower than $\sim 6.5 \times 10^3$ K is the most plausible source. The observed spectral energy distribution (SED) from the optical to ultraviolet can be expressed by a model consisting of a power-law component and an irradiated disk component.

Key words: Black hole physics — X-rays: binaries — X-rays: individual (V404 Cygni)

1. Introduction

On 2015 June 15, V404 Cygni started an outburst after 26 years of quiescence. The burst was detected and reported by Swift/BAT and MAXI (Barthelmy et al. 2015, Negoro et al. 2015).

In contrast to typical black hole transients, which exhibit a fast rise and exponential decay profile during an outburst, V404 Cygni showed multiple flaring activity in optical to γ-ray band during the outburst (Tanaka and Shibazaki. 1996, Ferrigno et al. 2015). The nature of the optical variation is still under discussion.

Kimura et al. (2016) argued that the source of the optical emission is mainly the outer disk irradiated by X-ray emission generated in the inner disk. This idea is also supported by Muñoz-Darias et al. (2016). An altanative scenario that relativistic non-thermal emission (jet) component combined with the accretion disk emission contributes to the optical light, is proposed by Marti et al. (2016), Tanaka et al. (2016), Gandhi et al. (2016), Lipunov et al. (2016), and Shahbaz et al. (2016).

In this paper, we present the multi-color optical light curves obtained using with the MITSuME instrument and results of the spectral-timing analysis.

2. Light Curve of V404 Cyg

Fig.1 shows the optical (g', R_C, and I_C-band) light curves during MJD 57192–57194, corresponding to the 4–6 days after the detection of X-ray outburst on MJD 57188. Variation on MJD 57192 seems to be composed of two distinct fluctuations; big-slow swings and small-fast wiggles. On the other hand, in MJD 57193 and 57194, fast drops in flax rather than big-slow swings were seen, while small wiggles remained. In all these variations, the fluxes in the optical three bands were always well correlated.

3. Analysis and results

3.1. Color-color Diagram

A color-color diagram is helpful to categorize the observed flux variation and to test the applicability of assumed emission models. We therefore calculated the spectral indices between g'-band and R_C-band (α_{gr}), and R_C-band and I_C-band (α_{ri}) for all the data point in Fig.1 and presented them in a color-color diagram (Fig.2). When converting the observed magnitudes to intrinsic fluxes F_ν, we adopted $A_V = 3.3$ and $R_V = A_V/E(B-V)=2.8$. The result is drawn by grey points in Fig.2. The grey dashed line and black dashed line trace loci for power-law spectra with different spectral indices and single temperature black body with different temperatures, respectively, whereas the black line and black-edged white line represents those for standard disk blackbody and irradiated disk blackbody (p=3/4: Shakura & Sunyaev 1973, and p=1/2: King & Ritter 1998) for different inner/outer-most temperatures under the condition that the disk temperature cannot across the critical temperature ~ 5000 K where the disk would

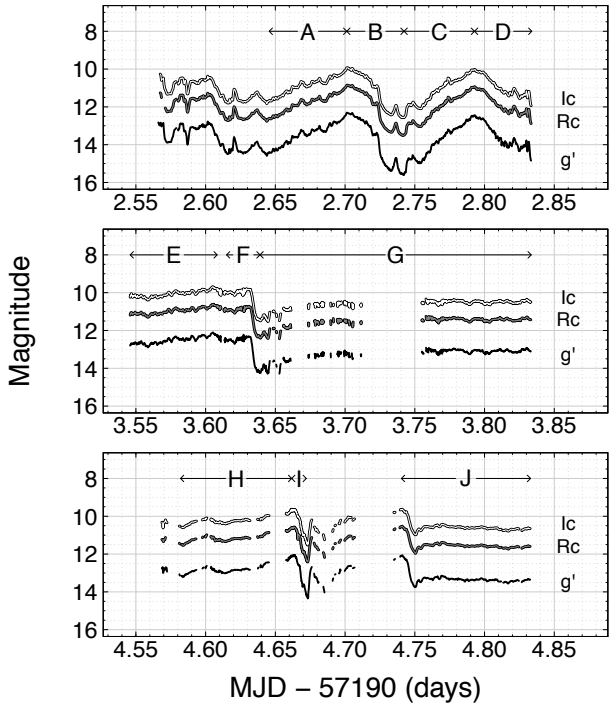

Fig. 1. The observed g′, R_C, and I_C light curves of V404 Cyg in MJD 57192–57194.

be unstable (King & Retter 1998, Życki et al. 1999), respectively. Here, p is the gradient index of the surface temperature of the accretion disk (T) when expressed as a function of the radial distance from the center (r); *i.e.* $T \propto r^{-p}$ (*e.g.* Mineshige et al. 1994).

Apparently, the points in the color-color diagram does not trace any of the model lines. It indicates that the optical variation cannot be attributed to a single emission component that can be expressed by a single-temperature or multi-temperature blackbody, or power-law model.

3.2. Flux-flux Plot

Using the color-color diagram, we showed that the optical variation of V404 Cyg cannot be attributed to changes of a parameter of a single emission mechanism. In this section, we further investigate the properties of the optical behavior phenomenologically on the flux-flux plot.

Examples of flux-flux plots are shown in Fig.3 with linear and broken linear model fits for the same data segments in the upper and lower panels respectively. The three columns correspond to the episode containing drastic flux declines: MJD = 57192.70 – 57192.74 (B), 57193.61 – 57193.64 (F), and 57194.66 – 57194.67 (I). We adopt a broken-linear model to express the behavior of the data on the flux-flux plot, since the broken-liner

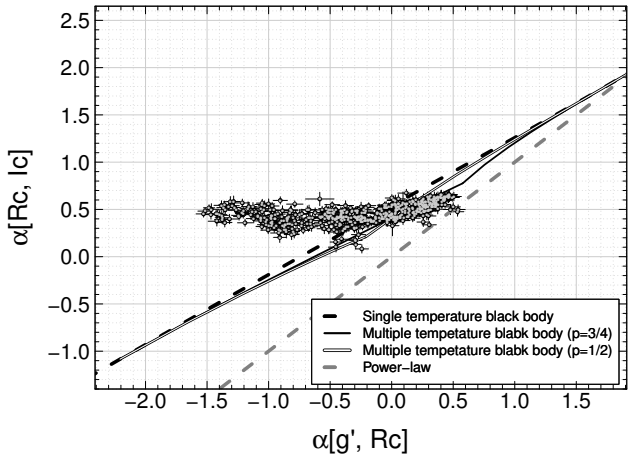

Fig. 2. Color-color diagram for the data in Fig.1 with the spectral indices between g′-band and R_C-band, and R_C-band and I_C-band.

model fits gives significantly small χ^2 values. Two linear branches below and above the break imply the existence of two variable components with distinct spectral indices α because the slope of the linear model on the flux-flux plot corresponds to $(\nu_2/\nu_1)^\alpha$.

To derive slopes for the two branches, we fitted a broken-linear model to the data in entire periods A–J. We found in flux-flux plots (*e.g.* Fig.3) that the dynamic range of the flux variation in the component above the break is lager than that below. It indicates that one variable component has quite large variability and dominates the optical variation when the component is much brighter than another one. Therefore, we named the components dominating above the break as "highly-variable component" (HVC) and the one below as "less-variable component" (LVC).

3.3. Decomposed Color-color Diagram

Fig.4 shows the color-color diagram for the decomposed components; HVC and LVC. The spectral indices of the HVC lie on the gray dashed line indicating power-law spectra with variable indices. On the other hand, those of the LVC are consistent with emission from the standard disks (p=3/4) with innermost temperatures ($T_{\rm in}$) of typically $\sim 1.5 \times 10^4$ K and 5000 K at the outer edge ($T_{\rm out}$), or irradiated disks (p=1/2) with $T_{\rm in} \gtrsim 2 \times 10^4$ K and $T_{\rm out} \lesssim 6500$ K.

4. Discussion

4.1. Optical Emission Components

We have shown that the optical variation is decomposed to two components; less-variable component (LVC) and highly-variable component (HVC). HVC has larger amplitude (∼5–10 times larger than that of LVC) and bluer

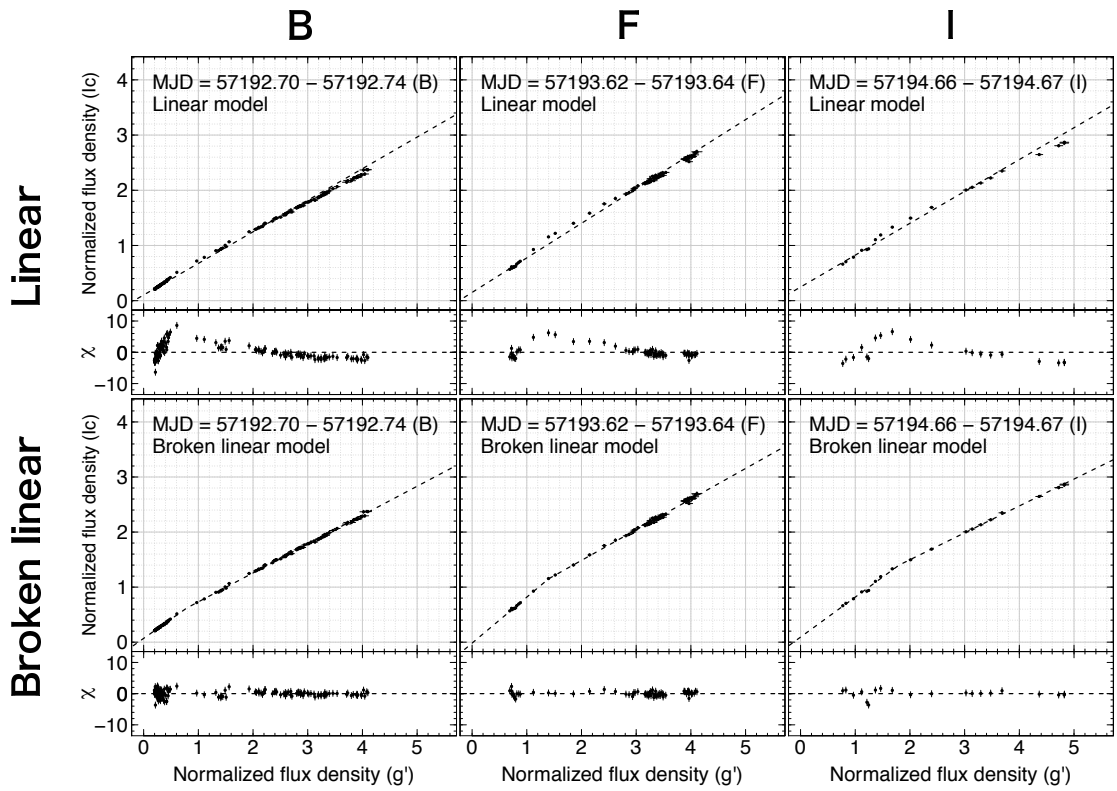

Fig. 3. The examples of flux-flux plot with the fluxes between g′-band and I_C-band. The upper panels are those fitted with a liner model, while the lower panels are fitted with a broken liner model.

color, and thus corresponds to "big-slow swings". On the other hand, LVC which has a redder spectrum corresponds to a characteristic behaviors mentioned as "small-fast wiggles". The latter is similar to "heartbeat-type" oscillations observed by Kimura et al. (2016), considering its small amplitude and its dominance at the low flux phase.

4.2. The emission origin of LVC

We found that spectral indices of LVC are consistent with those of a standard disk or an irradiated disk. However, a standard disk truncated at such a low innermost temperature ($\sim 1.5\times10^4$ K) seems to be difficult to reconcile with the detection of a disk component in the soft X-ray band (Radhika et al. 2016 and Walton et al. 2016). For the origin of LVC, thus, the irradiated disk is favored. From the observed flux, the outer radius of the disk is evaluated to be $\sim$ 3–5 $\times10^5$ Schwarzschild radius. It is consistent with the size limit based on the timescale of LVC. The irradiated disk is therefore the most plausible source of the LVC.

4.3. The emission origin of HVC

The decomposed color-color diagram shows that the spectra of HVC follow power-law models with spectral indices of $\sim$ 0.6–1.0.

Since the break of a jet spectrum between the optically thick and thin regions is expected to lie at $\sim$ 1.4–4.7 $\times10^{14}$ Hz (Shahbaz et al. 2016, Tanaka et al. 2016, and Itoh et al. 2016), the blue spectrum seen in HVC ($\alpha \sim$ 0.5–1.0) is possibly attributed to the transitioning spectrum from optically thick synchrotron spectrum (α = 2.5) to thin one. The jet is therefore one of the candidate of the origin of HVC.

Another possibility is the cyclo-synchrotron emission as proposed for XTE J1118+480 (Merloni et al. 2000 and Kanbach et al. 2001) and V4641 Sgr (Uemura et al. 2002). The self absorbed regime of the cyclo-synchrotron spectrum also can produce the hard spectral index than $\sim$0.6. The cyclo-synchroron emission is also one of the possible interpretation of the power-law component (HVC).

4.4. SED from optical to UV

To confirm our interpretation, we tried to describe the spectral energy distribution (SED) from optical to ultraviolet with a power-law and a irradiated disk spectrum. Constructed SED at MJD 57194.616 (included in "H" portion) are displayed in Fig.5. Four *S*wift/UVOT data (V, U, UVW1, and UVW2) are obtained quasi-

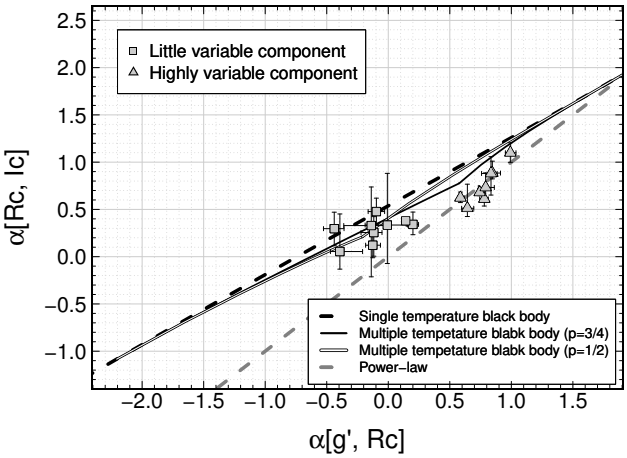

Fig. 4. Color-color diagram with the spectral indices between g′-band and R_C-band, and R_C-band and I_C-band, after the decomposition.

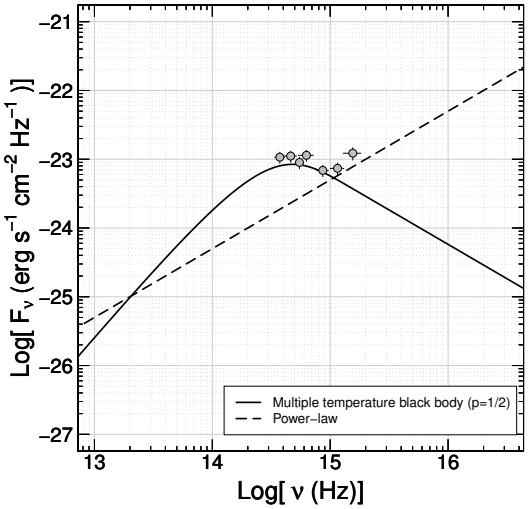

Fig. 5. SED from optical to UV with an irradiated disk spectrum (solid line) and power-law spectrum (dashed line) in MJD $\sim$ 57194.61 – 57194.62 (included in "H" period in Fig. 1).

simultaneously. The solid line and the dashed line denote the irradiated disk spectrum (temperature $T_{\rm out} = 5\times10^3$ K with the size of the emission region $R = 4 \times 10^5$ R_s) and power-law spectrum with the index $\alpha = 1.0$ respectively. Although we did not use the UVOT data for determination of the spectral model, all data points including the UV excess appear to be explainable by the two component model.

5. Summary

In this work, we found that the optical emission of V404 Cygni in the 2015 outburst can be decomposed to three components: the less-variable component (LVC), the highly-variable component (HVC), and the stable component, based on the flux-flux plots which is well represented by broken-liner expressions.

The decomposed spectral indices of LVC and HVC on the color-color diagram are consistent with those of multi-temperature black body spectra whose local temperature $T(r)$ is proportional to $r^{-1/2}$ and a power-law spectra, respectively.

The inner- and outer-most temperatures ($T_{\rm in/out}$) and the outermost radius of the irradiated disk are $T_{\rm in} \gtrsim 2.0 \times 10^4$ K, $T_{\rm out} \lesssim 6.5 \times 10^3$ K, and (3–5) $\times10^4$ Schwarzschild radius respectively. The index of the power-law component is $\sim$0.6–1. We proposed a non-thermal jet or a cyclo-synchrotron emission as the origin of the power-law component (HVC). The validity of our interpretation is supported by the spectral energy distribution from optical to UV with an irradiated disk and a power-law spectrum.

Our interpretation that the optical variation consists of two variable components, presents a possible solution for the problem pointed out by previous papers. Kimura et al. (2016) presented a problem about the amplitudes of the variations in X-ray and optical which are generally correlated; the X-ray flux variations were much larger than the optical ones. The smaller amplitude in the optical-band compared to X-ray is naturally explained by the "bias" (LVC and/or the stable component) underlying the component (HVC) correlated to X-ray variation.

References

Barthelmy S. D. et al. 2015, ATel, 17929, 1
Ferrigno C. et al. 2015, ATel, 7662, 1
Gandhi P. et al., 2016, MNRAS, 459, 554
Itoh R. et al. 2016, ArXiv, e-prints 1612.07513
Kanbach G., et al., 2001, Nature, 414
Kimura M. et al. 2016, Nature, 529, 54
King A. R. and Ritter, H. 1998, MNRAS, 293, L42
Lipunov V. M. et al., 2016, ArXiv, e-prints 1608.02764
Marti J. et al. 2016, A&A, 281, 1094
Merloni A., et al., 2000, MNRAS, 318, L15
Mineshige S. et al. 1994, ApJ, 426, 308
Muñoz-Darias et al. 2016, Nature, 534, 75
Negoro H. et al. 2016, ATel, 7646, 1
Radhika D. et al., 2016, ArXiv, e-prints 1601.03234
Shahbaz T. et al., 2016, MNRAS, 463, 1822
Shakura N. I., Sunyaev R. A., 1973, A&A, 24, 337
Tanaka Y. & Shibazaki, N., 1996, X-ray novae. Annu. Rev. Astron. Astrophys. 34, 607
Tanaka Y. T. et al., 2016, ApJ, 823, 35
Uemura M. et al., 2002, PASJ, 54, L79
Walton D. J. et al. 2016, ArXiv, e-prints 1609.01293
Życki P. T. et al., 1999, MNRAS, 309, 561